
OPTIMAL VACCINATION STRATEGIES IN THE CONTROL OF AN INFECTIOUS DISEASE: A SEIRV MODEL FOR ADMINISTRATION OF TWO VACCINES

A PREPRINT

• **Nelson L. Santos Junior**
Department of Mathematics
Federal University of Pernambuco
Recife, Pernambuco, Brazil
nelson.leal@ufpe.br

• **João A. M. Gondim**
Department of Mathematics
Federal University of Pernambuco
Recife, Pernambuco, Brazil
joao.gondim@ufpe.br

November 8, 2024

ABSTRACT

In this paper, we study the optimal control for an SEIR model adapted to the vaccination strategy of susceptible individuals. There are factors associated with a vaccination campaign that make this strategy not only a public health issue but also an economic one. In this case, optimal control is important as it minimizes implementation costs. We consider the availability of two vaccines with different efficacy levels, and the control indicates when each vaccine should be used. The optimal strategy specifies in all cases how vaccine purchases should be distributed. For similar efficacy values, we perform a sensitivity analysis on parameters that depend on the intrinsic characteristics of the vaccines. Additionally, we investigate the behavior of the number of infections under the optimal vaccination strategy.

Keywords Vaccination Strategy · SEIRV Model · Optimal Control · Contention Strategy

1 Introduction

In recent decades, mathematical models have become an important tool for investigating and predicting the dynamics of disease spread. These studies help us understand how different containment strategies should work [1]. Many epidemiological models have been pivotal in recent years, and the demand for developing such models was particularly high during the COVID-19 pandemic, an event that promises to be a historic milestone of the 21st century [2].

Vaccination is a containment strategy that significantly reduces the risk of infection, severe cases, hospitalization, and death, providing not only individual protection to vaccinated people, but also community-level protection [3]. It is estimated that in the case of COVID-19, a global reduction of 63% in total deaths was achieved during the first year of vaccination. In low-income countries, it is further estimated that the number of avoided deaths would increase by 111% if the vaccine coverage target of 40%, as established by the World Health Organization (WHO), had been met by each country by the end of 2021 [4].

Historically, many studies have focused on mathematical models of vaccination in the context of various diseases, such as hepatitis and measles [5], influenza [6], tuberculosis [7], and malaria [8]. Recently, numerous models have been developed to investigate different aspects of vaccination against SARS-CoV-2 during the COVID-19 pandemic, including vaccine distribution [9, 10], impact on the number of deaths [4, 11], sensitivity analysis of model parameters [12], the behavior of the basic reproductive number [13], and other related contexts.

Disease containment strategies generate financial costs for the government. For vaccination campaigns, for example, some of these costs are: purchase, storage, transportation, and distribution of vaccines, and installation of vaccination sites and medical staffing [14], in addition to investments in public awareness campaigns. Thus, a vaccination campaign is not only a public health measure but also a strategy with significant economic implications, and numerous studies

have sought to investigate this impact [14, 15, 16]. In this context, it is essential to develop mathematical models that examine containment strategies while managing associated economic costs, thereby providing insights to support government decisions in implementing these policies.

In epidemiological models, an optimal control problem can be used to define the ideal value of an important parameter of the model, so that it maximizes or minimizes a certain other variable present; then we can use optimal control to minimize a financial cost associated with a disease containment campaign. The theory of optimal control has been applied to disease models such as: HIV [17, 18, 19], tuberculosis [20, 21], influenza [22], and general epidemics [23, 24]. Recently, many studies have used optimal control for COVID-19 study [25, 26, 27, 28]. Gondim and Machado [29] used optimal control to analyze a SEIR model with quarantine of susceptible people which represents a total lockdown system during the COVID-19 pandemic. Santos Junior and Gondim [30] used optimal control to analyze a model for quarantine only of infected people which is closer to the proper definition of quarantine.

The goal of this paper is work with the optimal control on a SEIR model adapted for vaccination campaign of susceptible people with two types of vaccines, we will calculate numerically these controls for describe the ideal use a given type of vaccine, minimizing not only the number of infected people, but also the economic costs associated with the use of this vaccine. We hope that the results can suggest government decisions when implementing the vaccination campaigns. The results indicates when the government must use a vaccine or other depending of your efficacy, in this cases, we indicates the purchase percentage of each vaccine. When the two vaccines have efficacy values very near, we present a study of sensibility for those parameters that depend of other characteristic of vaccines. Finally, we analyze the number of infected in three contexts: when we only use the first vaccine, when we use both vaccines according optimal control and when we only use the second vaccine.

2 The epidemiology model

We will consider a modified SEIR model with a one-dose vaccination strategy for susceptible individuals. We know that in the case of COVID-19, for example, a vaccine with partial protection was sufficient to control the SARS-CoV-2 pandemic [31, 32], so we will work with vaccines that are not 100% effective. Here, we consider two vaccines, V_1 and V_2 , with efficacy θ_1 and θ_2 , respectively, where $\theta_2 < \theta_1 < 1$.

From [33], the efficacy θ_i , for $i = 1, 2$, is given by $\theta_i = (P - P_i)/P$, where P and P_i indicate the attack rates for unvaccinated and vaccinated individuals, respectively, i.e., the probability that a contact results in transmission. Thus, we have $P_i = P(1 - \theta_i)$ for $i = 1, 2$. From [34], the transmission rate in the SEIR model is $\beta = cP$, where c is the contact rate. Therefore, for vaccinated individuals, the transmission rate is given by $\beta_i = cP_i = cP(1 - \theta_i) = \beta(1 - \theta_i)$, meaning the vaccine efficacy directly reduces the transmission rate of the disease.

The efficacy values chosen for use in the simulations are motivated by real COVID-19 vaccine efficacies. For example, the Pfizer vaccine is 91% effective [35], the AstraZeneca vaccine is 74% effective [36], the Janssen vaccine is 67% effective [37], and the Coronavac vaccine is 51% effective [38]. These references are based on phase 3 trials in various countries with different population groups; some efficacies are guaranteed for two doses of the vaccine, but for simplicity, we assume these efficacies are valid for one dose of the vaccine in our study.

Let $S(t)$, $V_1(t)$, $V_2(t)$, $E(t)$, $I(t)$, and $R(t)$ be the numbers of susceptible individuals, individuals vaccinated with vaccine V_1 , individuals vaccinated with vaccine V_2 , exposed individuals, infected individuals, and recovered individuals, respectively. We assume that the total population

$$N(t) = S(t) + V_1(t) + V_2(t) + E(t) + I(t) + R(t)$$

is constant, as we are considering only a short time frame in comparison to the demographic time scale.

Vaccination was associated with high short-term protection against SARS-CoV-2, but this protection decreases considerably after a few months [39]. This strategy helps contain disease spread but does not completely eliminate the risk of infection, as reinfections post-vaccination have been reported [40, 41]. Therefore, our model includes the effect of a potential reinfection by the disease.

Figure 2 illustrates the dynamics between the compartments of our model.

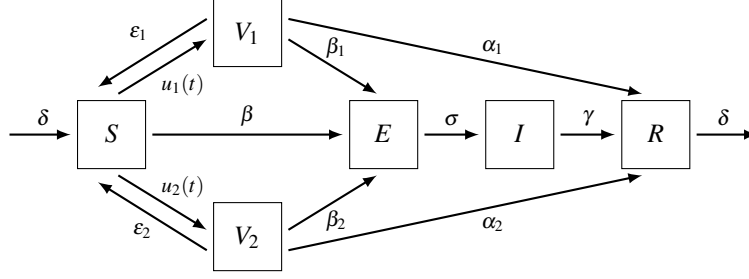


Figure 1: Compartment diagram of the model.

The susceptible population decreases when individuals move into the exposed class at a transmission rate β , are vaccinated with vaccine V_1 at a control rate $u_1(t)$, or are vaccinated with vaccine V_2 at a control rate $u_2(t)$. The controls represent the fraction of individuals vaccinated per unit time at t . Here, our boundary condition for the control is

$$0 \leq u(t) \leq 1, \quad (1)$$

since there is no maximum time to be vaccinated, and the minimum time is 1 day.

In the model, there are three possibilities for a vaccinated individual:

1. Leave the class of those vaccinated with immunity and move into the class of recovered people at a rate α_i , for $i = 1, 2$;
2. Being vulnerable after leaving the vaccinated class with possibility of contracting the disease, moving into the susceptible class to a rate ε_i , for $i = 1, 2$;
3. Contract the disease before leaving the vaccinated class becoming a exposed individual and transmitting the disease at a rate $\beta_i = 1 - \theta_i$, for $i = 1, 2$;

The exposed population decreases when individuals move into the infected class at a latency rate σ . The recovered population increases at an exit rate γ and decreases at a reinfection rate δ . Note that in this model, people can recover by acquiring vaccine-induced immunity without necessarily experiencing an infection.

The system of equations is

$$\left\{ \begin{array}{l} \frac{dS}{dt} = -\frac{\beta SI}{N} - u_1(t)S - u_2(t)S + \varepsilon_1 V_1 + \varepsilon_2 V_2 + \delta R \\ \frac{dV_1}{dt} = u_1(t)S - \frac{\beta_1 V_1 I}{N} - \varepsilon_1 V_1 - \alpha_1 V_1 \\ \frac{dV_2}{dt} = u_2(t)S - \frac{\beta_2 V_2 I}{N} - \varepsilon_2 V_2 - \alpha_2 V_2 \\ \frac{dE}{dt} = \frac{\beta SI}{N} + \frac{\beta_1 V_1 I}{N} + \frac{\beta_2 V_2 I}{N} - \sigma E \\ \frac{dI}{dt} = \sigma E - \gamma I \\ \frac{dR}{dt} = \gamma I - \delta R + \alpha_1 V_1 + \alpha_2 V_2 \end{array} \right. \quad (2)$$

All parameters are nonnegative and were taken from [13], where the Bayesian Markov Chain Monte Carlo (MCMC) method [42] shows the convergence of the parameters. In that reference, only one vaccine is considered, providing a single value for the immunity rate and for the rate of return to the susceptible class. In our study, we incorporate two vaccines, and we need two values for each parameter. For simplicity, we initially assume $\alpha_1 = \alpha_2$ and $\varepsilon_1 = \varepsilon_2$. The parameter values for our numerical simulations are described in Table 1.

Table 1: Parameters values.

Parameter	Description	Value
β	transmission rate	0.45
σ	latency rate	0.25
γ	recovered rate	0.07
δ	reinfection rate	0.65
α_1	V_1 vaccine immunity rate	0.08
α_2	V_2 vaccine immunity rate	0.08
ε_1	rate of return to susceptible class of V_1 vaccine	0.54
ε_2	rate of return to susceptible class of V_2 vaccine	0.54

The number of susceptible individuals is considered equal to the total population, as the proportion of exposed, infected, and recovered individuals is very small in comparison to the total population, as in [29]. We assume that there are no vaccinated individuals at the start of the simulation. Our initial time point uses data from Brazil as of May 8, 2020 [29, 43]. The number of recovered individuals is calculated as the difference between the total number of cases and the number of deaths. The mean incubation period of the disease is estimated to be around 5 days [44], so the number of exposed individuals is determined by subtracting the number of active cases on May 8 from the number of active cases on May 13. The initial conditions are described in Table 2.

Table 2: Description of initial conditions.

Group	Initial Condition
Susceptible	200000000
Vaccinated with V_1 vaccine	0
Vaccinated with V_2 vaccine	0
Exposed	65124
Infected	76603
Recovery	65124

3 The optimization problem

Following system (2), we minimize the functional

$$J = \int_0^T (I(t) + B_1 u_1^2(t) + B_2 u_2^2(t)) dt. \quad (3)$$

In the formula (3), T is the duration of vaccination and the parameters B_1 and B_2 are the costs of implementation of V_1 and V_2 vaccines, respectively. We assume that $B_1, B_2 > 0$, as well as that

$$B = B_1 + B_2, \quad (4)$$

where B is the total control cost.

Sufficient conditions for the existence of optimal controls follow from standard results from optimal control theory, we can use Theorem 2.1 in Joshi et al. [45] to show that the optimal control exists.

Pontryagin's maximum principle [46, 47] establish that optimal controls are solutions of the Hamiltonian system with Hamiltonian function

$$\begin{aligned}
H = & I + B_1 u_1^2 + B_2 u_2^2 + u_1 S(\lambda_{V_1} - \lambda_S) + u_2 S(\lambda_{V_2} - \lambda_S) \\
& + \frac{\beta SI}{N} (\lambda_E - \lambda_S) + \frac{\beta_1 V_1 I}{N} (\lambda_E - \lambda_{V_1}) + \frac{\beta_2 V_2 I}{N} (\lambda_E - \lambda_{V_2}) \\
& + \varepsilon_1 V_1 (\lambda_S - \lambda_{V_1}) + \varepsilon_2 V_2 (\lambda_S - \lambda_{V_2}) + \alpha_1 V_1 (\lambda_R - \lambda_{V_1}) \\
& + \alpha_2 V_2 (\lambda_R - \lambda_{V_2}) + \sigma E (\lambda_I - \lambda_E) + \delta R (\lambda_S - \lambda_R) + \gamma I (\lambda_R - \lambda_I),
\end{aligned} \quad (5)$$

involving the state variables S, V_1, V_2, E, I, R and the adjoint variables $\lambda_S, \lambda_{V_1}, \lambda_{V_2}, \lambda_E, \lambda_I, \lambda_R$, which satisfy the adjoint system (6).

$$\begin{cases} \frac{d\lambda_S}{dt} = \frac{I}{N^2} \left[\beta_1 V_1 (\lambda_E - \lambda_{V_1}) + \beta_2 V_2 (\lambda_E - \lambda_{V_2}) + \beta (N - S) (\lambda_S - \lambda_E) \right] \\ \quad + u_1 (\lambda_S - \lambda_{V_1}) + u_2 (\lambda_S - \lambda_{V_2}) \\ \frac{d\lambda_{V_1}}{dt} = \frac{I}{N^2} \left[\beta S (\lambda_E - \lambda_S) + \beta_2 V_2 (\lambda_E - \lambda_{V_2}) + \beta_1 (N - V_1) (\lambda_{V_1} - \lambda_E) \right] \\ \quad + \varepsilon_1 (\lambda_{V_1} - \lambda_S) + \alpha_1 (\lambda_{V_1} - \lambda_R) \\ \frac{d\lambda_{V_2}}{dt} = \frac{I}{N^2} \left[\beta S (\lambda_E - \lambda_S) + \beta_1 V_1 (\lambda_E - \lambda_{V_1}) + \beta_2 (N - V_2) (\lambda_{V_2} - \lambda_E) \right] \\ \quad + \varepsilon_2 (\lambda_{V_2} - \lambda_S) + \alpha_2 (\lambda_{V_2} - \lambda_R) \\ \frac{d\lambda_E}{dt} = \frac{I}{N^2} \left[\beta S (\lambda_E - \lambda_S) + \beta_1 V_1 (\lambda_E - \lambda_{V_1}) + \beta_2 V_2 (\lambda_E - \lambda_{V_2}) \right] \\ \quad + \sigma (\lambda_E - \lambda_I) \\ \frac{d\lambda_I}{dt} = \frac{N - I}{N^2} \left[\beta S (\lambda_S - \lambda_E) + \beta_1 V_1 (\lambda_{V_1} - \lambda_E) + \beta_2 V_2 (\lambda_{V_2} - \lambda_E) \right] \\ \quad + \gamma (\lambda_I - \lambda_R) - 1 \\ \frac{d\lambda_R}{dt} = \frac{I}{N^2} \left[\beta S (\lambda_E - \lambda_S) + \beta_1 V_1 (\lambda_E - \lambda_{V_1}) + \beta_2 V_2 (\lambda_E - \lambda_{V_2}) \right] \\ \quad + \delta (\lambda_R - \lambda_S) \end{cases} \quad (6)$$

The adjoint variables also must satisfy the transversality conditions

$$\lambda_S(T) = \lambda_{V_1}(T) = \lambda_{V_2}(T) = \lambda_E(T) = \lambda_I(T) = \lambda_R(T) = 0. \quad (7)$$

Finally, the optimality conditions come from solving

$$\left. \frac{\partial H}{\partial u} \right|_{u=u^*} = 0,$$

this results in

$$u_i^* = \frac{S(\lambda_S - \lambda_{V_i})}{2B_i}, \quad i = 1, 2. \quad (8)$$

Since we are considering bounded controls, by (1) the optimal control u^* are calculated [47] using

$$u^* = \min \left\{ 1, \max \left\{ 0, \frac{S(\lambda_S - \lambda_{V_i})}{2B_i} \right\} \right\}, \quad i = 1, 2. \quad (9)$$

Uniqueness of the optimal controls (at least for small enough T) also follow from standard results, such as Theorem 2.3 in Joshi et al. [45].

The numerical solutions of systems (2) and (6) can be found using the forward-backward sweep method [47]. We have a initial condition in $t = 0$ for system (2) and a initial condition in $t = T$ for system (6), the algorithm of sweep uses these conditions and works with the following steps:

Step 1: Starts with an initial guess of the controls u_1 and u_2 , solves (2) using the initial condition for state variable and the values for u_i forward in time;

Step 2: Uses initial condition (7) and the results provided in Step 1 for the state variables and for the optimal control, to solve (6) backward in time, the new controls are defined by (9);

Step 3: This process continues until a convergence is obtained.

4 Discussion

Our optimal control problem depends on the implementation costs B_1 and B_2 of the two vaccines V_1 and V_2 , respectively. Here, the costs for the vaccines will be distributed as $B_i = \theta_i \cdot 10^4$ for $i = 1, 2$; i.e., the implementation cost of a vaccine is proportional to its efficacy power. This decision was made due to the difficulty of finding specific references on government spending for vaccine procurement.

Next, see the plots the graphs of the optimal controls $u_1(t)$ and $u_2(t)$ for vaccination durations of 60, 120, and 180 days. In all cases, u_1 represents the implementation of the vaccine with higher efficacy, therefore, higher cost.

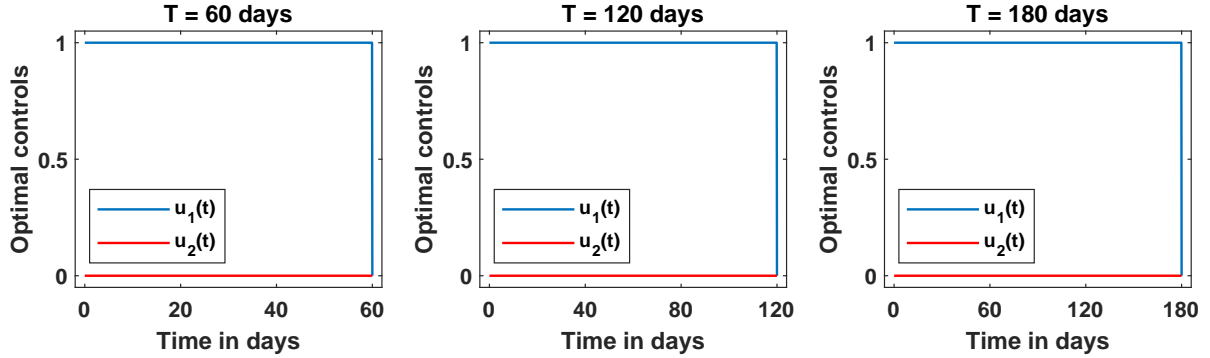


Figure 2: The optimal controls for use of vaccines with effectiveness of 91% and 51% for different vaccination campaigns lengths.

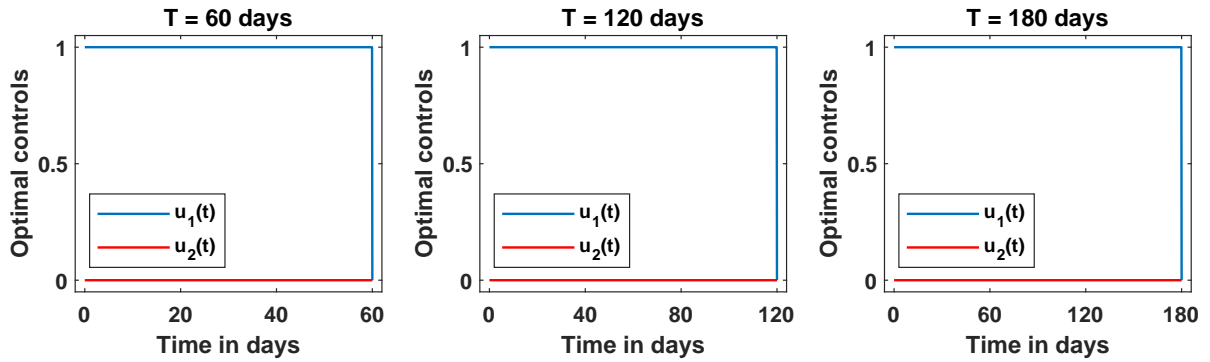


Figure 3: The optimal controls for use of vaccines with effectiveness of 74% and 51% for different vaccination campaigns lengths.

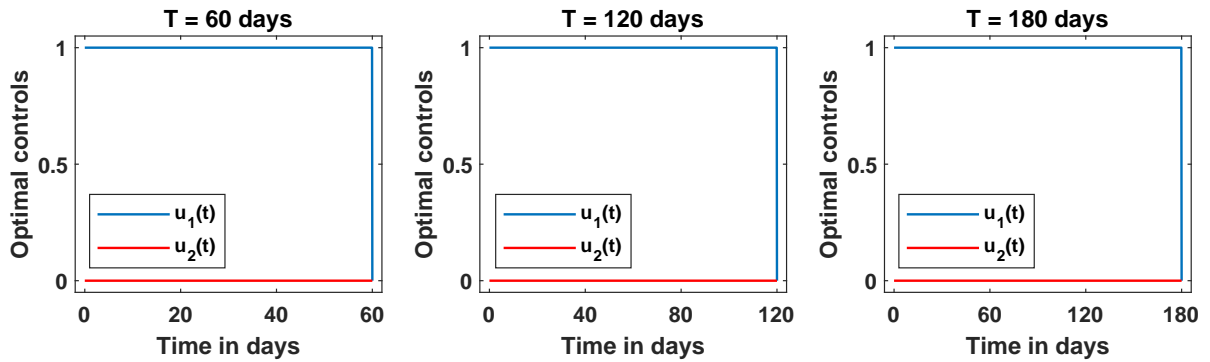


Figure 4: The optimal controls for use of vaccines with effectiveness of 67% and 51% for different vaccination campaigns lengths.

In Figures 2, 3, and 4, regardless of the higher economic cost, the optimal control suggests prioritizing the use of the V_1 vaccine with an efficacy of 91%, 74%, or 67% over the V_2 vaccine, which has an efficacy of 51%. This preference is likely due to the impact of the vaccine's efficacy on reducing the disease transmission rate. Specifically, for vaccinated individuals, the transmission rate decreases linearly, as shown in Figure 5. In this context, note that $\beta_2 = 0.2378$, while smaller than the usual rate for unvaccinated individuals, $\beta = 0.45$, remains significantly higher than $\beta_1 = 0.1601$, $\beta_1 = 0.1262$, or $\beta_1 = 0.0436$.

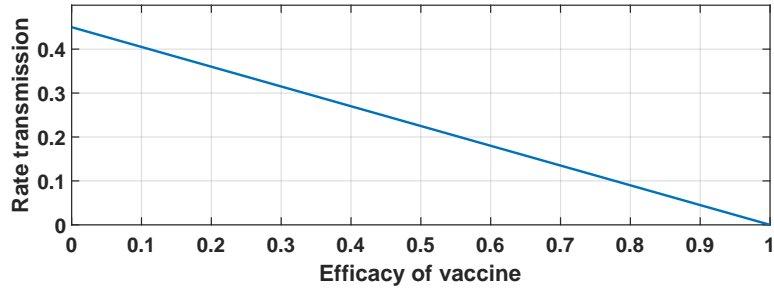


Figure 5: Behavior of rate transmission for vaccinated people.

In Figures 6, 7 and 8 see the curve of vaccinated for the controls of the Figures 2, 3 and 4, respectively. The number of vaccinated people with the V_2 vaccine is practically zero when compared to the size of the susceptible population, this is an expected result considering what we saw in the plots of the optimal controls. After this discussion, it is recommended that the government purchase only the most effective vaccine, a vaccine with an efficacy of 51% only be recommended if it is the only one available.

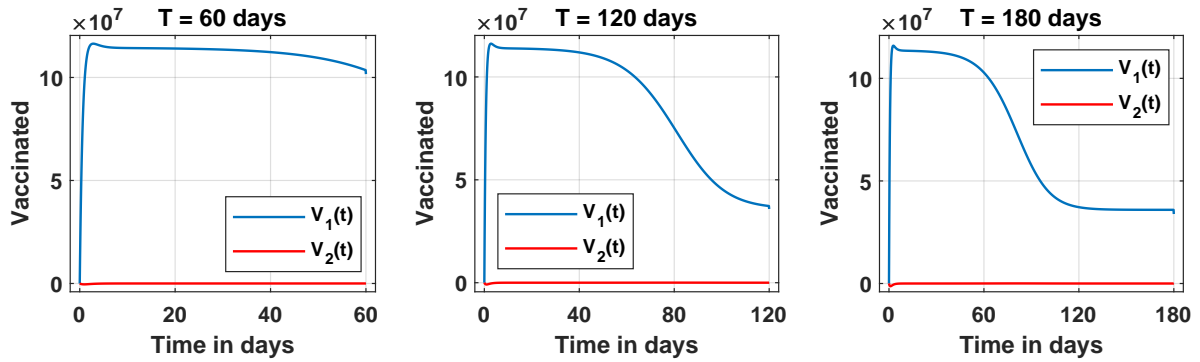


Figure 6: Vaccination curves for the use of vaccines with effectiveness of 91% and 51% for different vaccination campaign lengths.

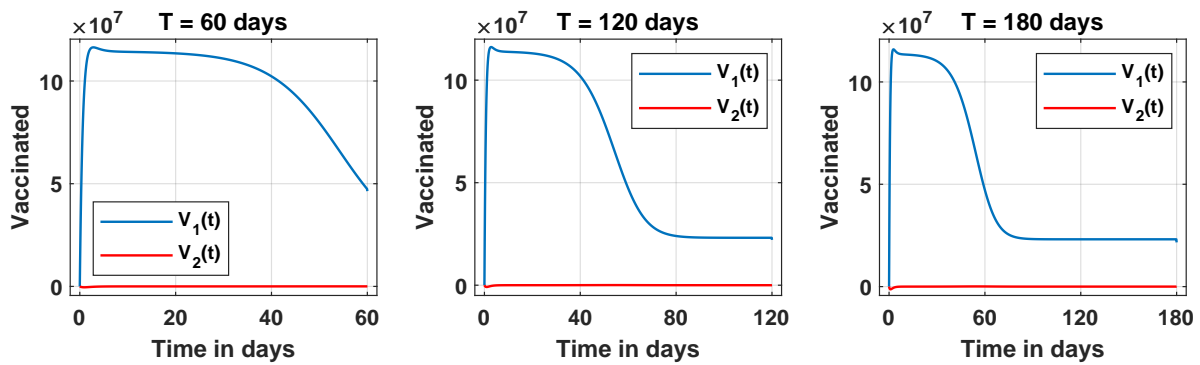


Figure 7: Vaccination curves for the use of vaccines with effectiveness of 74% and 51% for different vaccination campaign lengths.

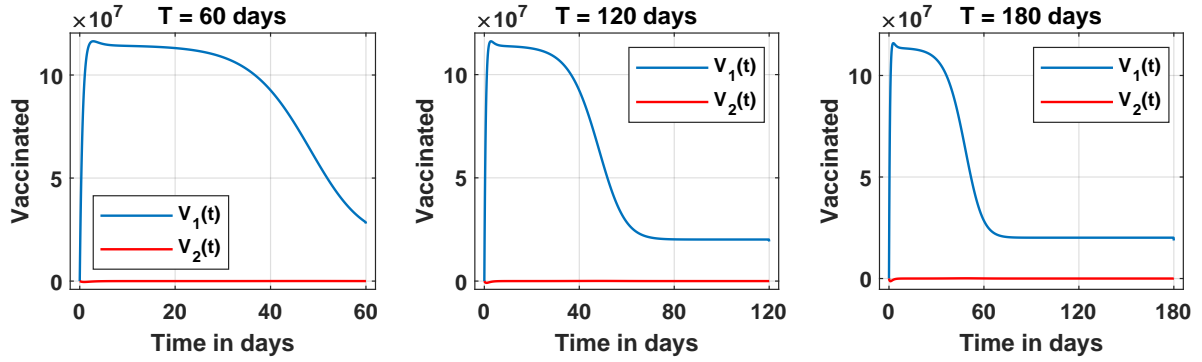


Figure 8: Vaccination curves for the use of vaccines with effectiveness of 67% and 51% for different vaccination campaign lengths.

In Figure 9, for most of the campaign duration, the optimal control suggests using the V_1 vaccine with 91% efficacy compared to the V_2 vaccine with 74% efficacy. However, there is a simultaneous use of both vaccines starting on days 51, 109, and 169 for vaccination campaigns lasting 60, 120, and 180 days, respectively. When the V_2 vaccine has 67% efficacy, as shown in Figure 10, the optimal control behavior remains almost identical to that in Figure 9, with simultaneous use of both vaccines beginning on days 57, 116, and 176 for vaccination campaigns lasting 60, 120, and 180 days, respectively.

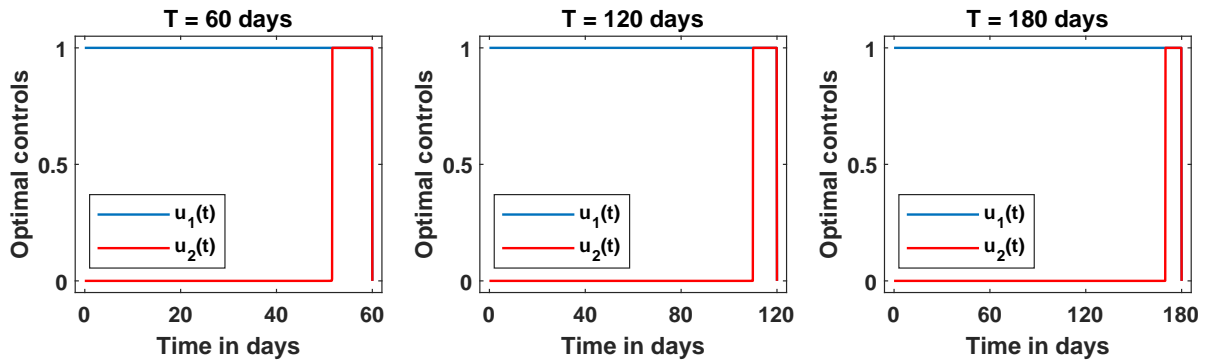


Figure 9: The optimal controls for the use of vaccines with effectiveness of 91% and 74% for different vaccination campaign lengths.

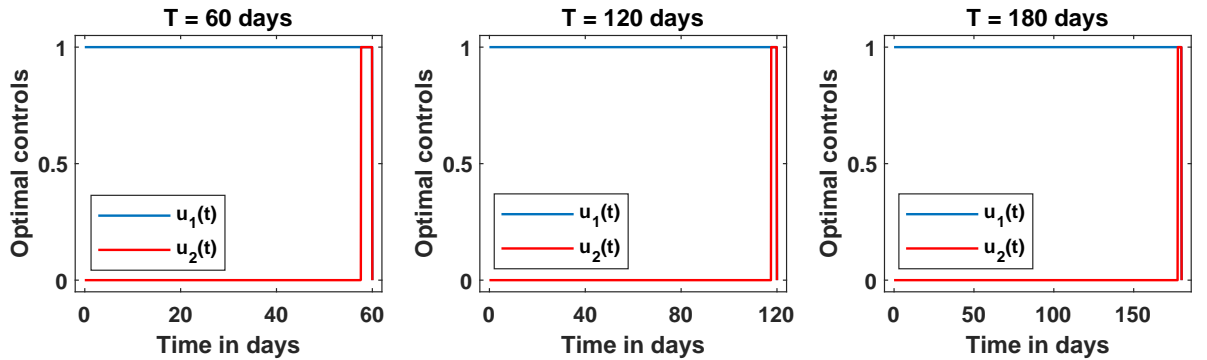


Figure 10: The optimal controls for use of vaccines with effectiveness of 91% and 67% for different vaccination campaign lengths.

We understand that the strategy of the optimal controls in Figures 9 and 10 seeks to balance economic expenses, given that the V_2 vaccine has a lower implementation cost. Additionally, the lower effectiveness of the V_2 vaccine is

unlikely to pose issues, as the population has likely already achieved herd immunity through the initial administration of the more effective V_1 vaccine.

In Figures 11 and 12, see the curve of vaccinated individuals based on the controls shown in Figures 9 and 10. See that due to the use of the V_2 vaccine indicated by control, there is an increase in the number of people vaccinated with this vaccine in the final days of the campaign.

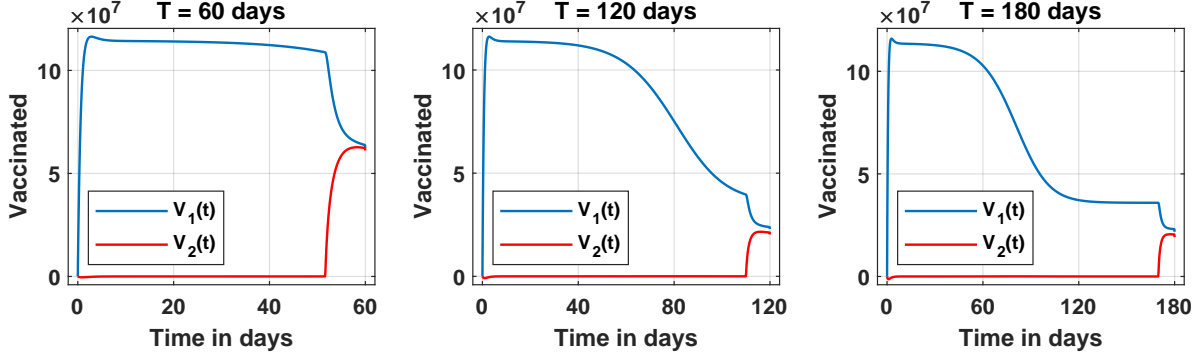


Figure 11: Vaccination curves for the use of vaccines with effectiveness of 91% for 74% for different vaccination campaign lengths.

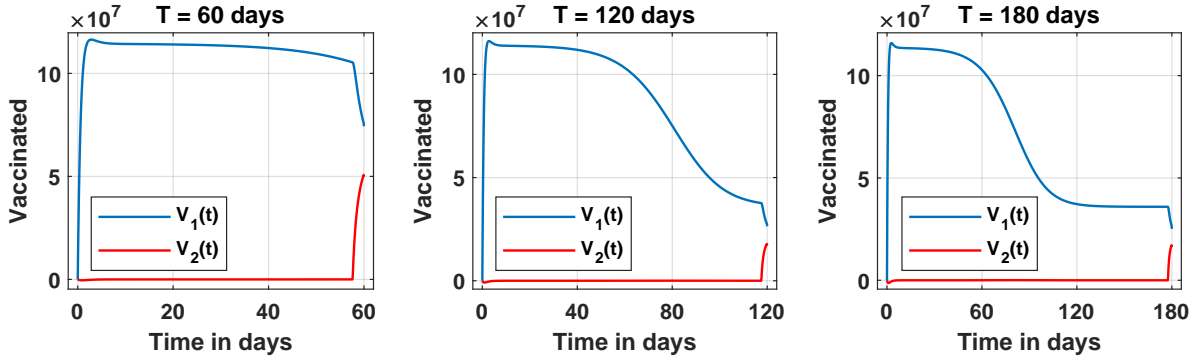


Figure 12: Vaccination curves for the use of vaccines with effectiveness of 91% and 67% for different vaccination campaign lengths.

Using the Trapezoidal rule for numerical integration [48], we calculated the integral of the vaccination curves $V_1(t)$ and $V_2(t)$ to determine the quantity of vaccines used during the campaign, providing a recommended distribution for government agencies to guide vaccine procurement.

Table 3: Distribution for vaccine procurement according to Figure 11.

Vaccine	T = 60 days	T = 120 days	T = 180 days
V_1	93,44 %	98,18 %	98,55 %
V_2	6,66 %	1,82 %	1,45 %

Table 4: Distribution for vaccine procurement according to Figure 12.

Vaccine	T = 60 days	T = 120 days	T = 180 days
V_1	98,77 %	99,70 %	99,76 %
V_2	1,23 %	0,30 %	0,24 %

For vaccines with 74% and 67% efficacy, there is a small difference between the efficacy rates θ_1, θ_2 and the transmission rates β_1, β_2 . In this case, as shown in Figure 13, the plot of optimal control is overlaid, indicating a simultaneous use of the vaccines throughout the duration of the vaccination campaign.

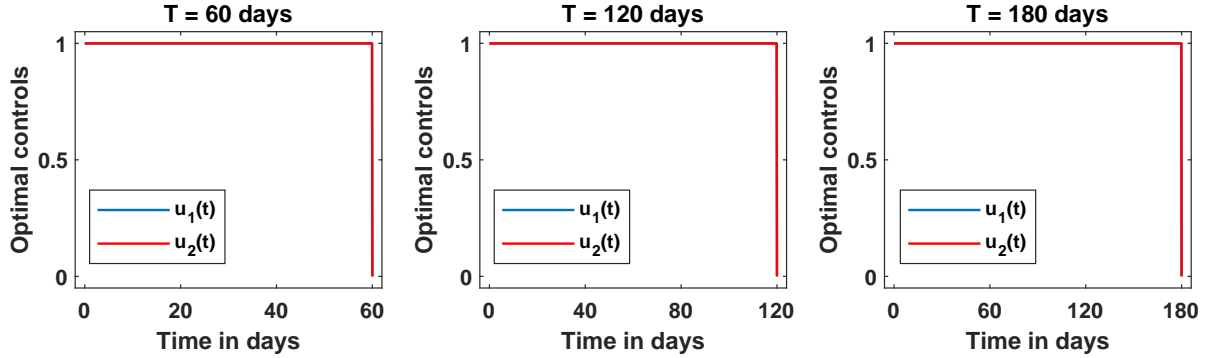


Figure 13: The optimal controls for use of vaccines with effectiveness of 74% and 67% and different vaccination campaigns lengths

See in Figure 14, the curve of vaccinated people based on the optimal control in Figure 13.

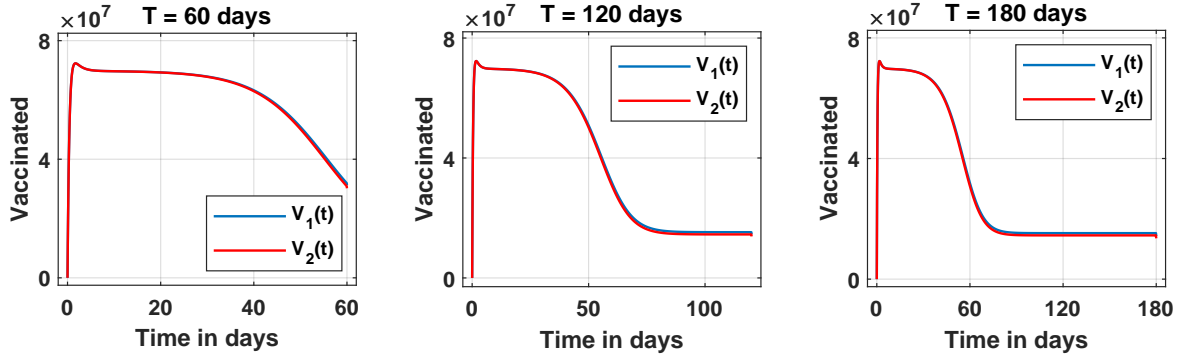


Figure 14: Vaccination curves for the use of vaccines with effectiveness of 74% and 67% and different vaccination campaigns lengths.

In all cases shown in Figure 14, the number of people vaccinated with the V_1 and V_2 vaccines remains practically the same throughout the vaccination period. In this context, we also calculate the integral of the vaccinated curves $V_1(t)$ and $V_2(t)$ to observe the quantity of vaccines used during the campaign, as presented in Table 5.

Table 5: Distribution for vaccine procurement according to Figure 14.

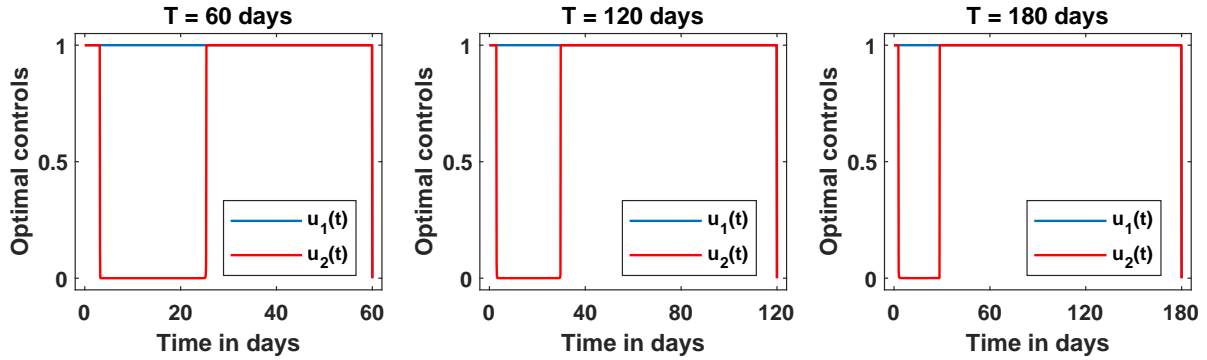
Vaccine	T = 60 days	T = 120 days	T = 180 days
V_1	50,11 %	50,34 %	50,48 %
V_2	49,89 %	49,66 %	49,52 %

We know that from Figure 13, the optimal control does not indicate preference for the use of one vaccine over another with the parameters adopted in Table 1. In this context, we investigated the sensitivity of the parameters related to the immunity rate, the rate of return to the susceptible class, and efficacy, which can vary in the real world according to the characteristics of the vaccines used.

Table 6: Values of α_1 , α_2 , ε_1 and ε_2 for sensibility analysis.

$\alpha_1 > \alpha_2$	$\varepsilon_1 > \varepsilon_2$	$\alpha_1 < \alpha_2$	$\varepsilon_1 < \varepsilon_2$	$\alpha_1 > \alpha_2$	$\varepsilon_1 < \varepsilon_2$	$\alpha_1 < \alpha_2$	$\varepsilon_1 > \varepsilon_2$
$\alpha_1 = 0.088$	$\varepsilon_1 = 0.594$	$\alpha_1 = 0.08$	$\varepsilon_1 = 0.54$	$\alpha_1 = 0.088$	$\varepsilon_1 = 0.54$	$\alpha_1 = 0.08$	$\varepsilon_1 = 0.594$
$\alpha_2 = 0.08$	$\varepsilon_2 = 0.54$	$\alpha_2 = 0.008$	$\varepsilon_2 = 0.594$	$\alpha_2 = 0.08$	$\varepsilon_2 = 0.594$	$\alpha_2 = 0.088$	$\varepsilon_2 = 0.54$
$\alpha_1 = 0.096$	$\varepsilon_1 = 0.648$	$\alpha_1 = 0.08$	$\varepsilon_1 = 0.54$	$\alpha_1 = 0.096$	$\varepsilon_1 = 0.54$	$\alpha_1 = 0.08$	$\varepsilon_1 = 0.648$
$\alpha_2 = 0.08$	$\varepsilon_2 = 0.54$	$\alpha_2 = 0.096$	$\varepsilon_2 = 0.648$	$\alpha_2 = 0.08$	$\varepsilon_2 = 0.648$	$\alpha_2 = 0.096$	$\varepsilon_2 = 0.54$
$\alpha_1 = 0.08$	$\varepsilon_1 = 0.54$	$\alpha_1 = 0.072$	$\varepsilon_1 = 0.486$	$\alpha_1 = 0.08$	$\varepsilon_1 = 0.486$	$\alpha_1 = 0.072$	$\varepsilon_1 = 0.54$
$\alpha_2 = 0.072$	$\varepsilon_2 = 0.486$	$\alpha_2 = 0.08$	$\varepsilon_2 = 0.54$	$\alpha_2 = 0.072$	$\varepsilon_2 = 0.54$	$\alpha_2 = 0.08$	$\varepsilon_2 = 0.486$
$\alpha_1 = 0.08$	$\varepsilon_1 = 0.54$	$\alpha_1 = 0.064$	$\varepsilon_1 = 0.432$	$\alpha_1 = 0.08$	$\varepsilon_1 = 0.432$	$\alpha_1 = 0.064$	$\varepsilon_1 = 0.54$
$\alpha_2 = 0.064$	$\varepsilon_2 = 0.432$	$\alpha_2 = 0.08$	$\varepsilon_2 = 0.54$	$\alpha_2 = 0.064$	$\varepsilon_2 = 0.54$	$\alpha_2 = 0.08$	$\varepsilon_2 = 0.432$

In Table 6, we vary the values of the parameters α_1 , α_2 , ε_1 , and ε_2 up and down by 10% and 20%, and the optimal controls were calculated for this set of values. For all percentage up variations, the optimal controls exhibit the same behavior as shown in Figure 13. For the down variations, there is one case of a change in control, which is illustrated in Figure 15.

Figure 15: Optimal controls for $\alpha_1 = 0.08$, $\alpha_2 = 0.064$, $\varepsilon_1 = 0.432$, $\varepsilon_2 = 0.54$.

In Figure 15, the reduction in the use of the V_2 vaccine is acceptable. Note that we have a reduction of 20% in the parameter values of α_2 and ε_1 . This change in parameters indicates that the V_2 vaccine has a smaller recovery power, while the V_1 vaccine shows a reduction in the number of people returning to the susceptible class. Furthermore, the 20% variation represents a threshold; that is, a reduction of 19% does not result in a change in the behavior of the optimal controls depicted in Figure 13.

For the control shown in Figure 15, the curve of vaccinated individuals is presented in Figure 16. We also calculate the integral of the curves of vaccinated to observe the quantity of vaccines used during the campaign, as detailed in Table 7.

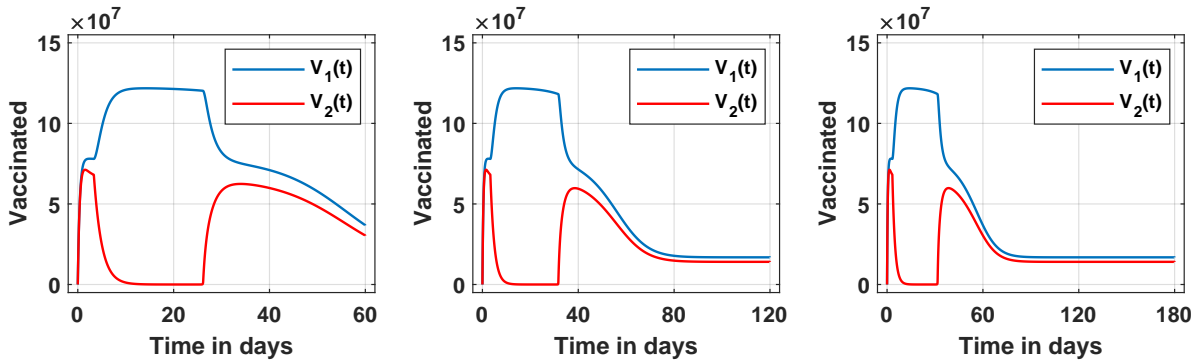
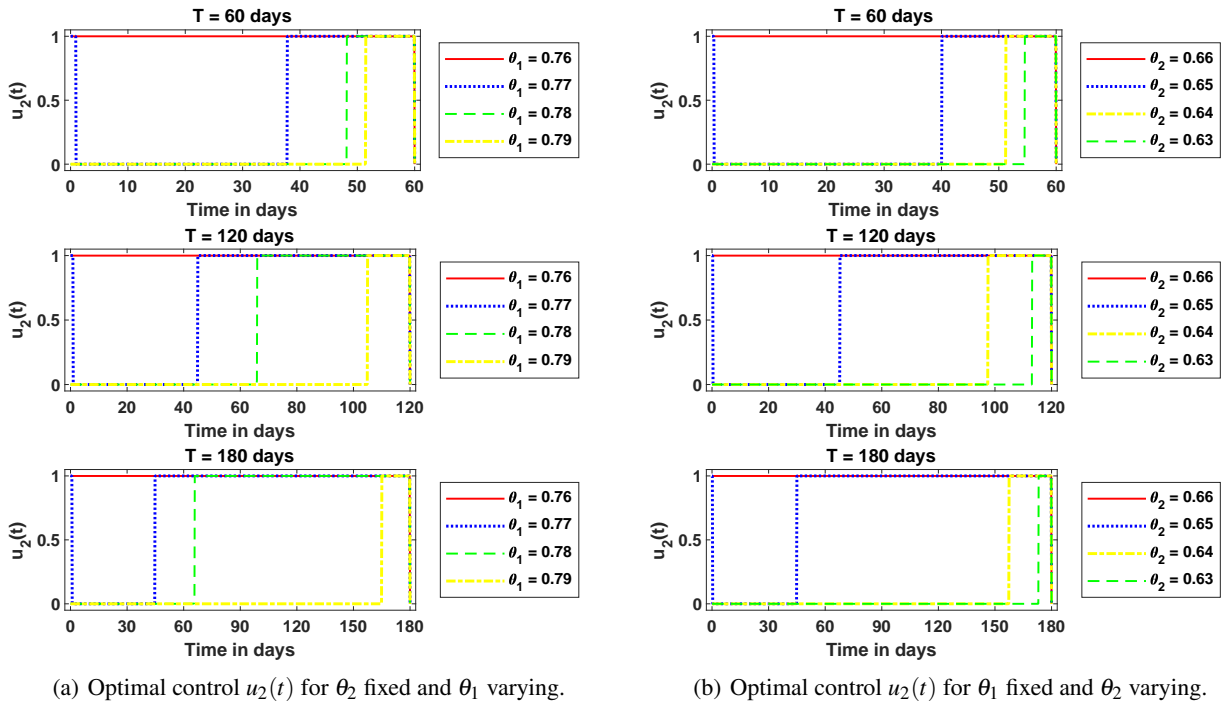
Figure 16: Vaccinated for $\alpha_1 = 0.08$, $\alpha_2 = 0.064$, $\varepsilon_1 = 0.432$, $\varepsilon_2 = 0.54$.

Table 7: Distribution for vaccine procurement according to Figure 15.

Vaccine	T = 60 days	T = 120 days	T = 180 days
V_1	71,60 %	71,21%	68,37 %
V_2	28,40 %	28,79%	31,63 %

We also vary the efficacy parameters θ_1 and θ_2 to conduct a sensitivity analysis of these parameters. The behavior of the optimal control $u_1(t)$, as seen in Figure 13, does not change, while the control $u_2(t)$ changes in the following way:

- Fixed $\theta_2 = 0.67$, the control $u_2(t)$ changes to values of θ_1 above $\theta_1 = 0.77$, this is shown in Figure 17(a);
- Fixed $\theta_1 = 0.74$, the control $u_2(t)$ changes to values of θ_2 below $\theta_2 = 0.65$, this is shown in Figure 17(b);

Figure 17: Sensibility analysis for efficacy parameters θ_1 and θ_2 .

In summary, as the efficacy parameters become closer, the simultaneous use of the vaccines is indicated. When the values diverge, the continued use of the V_1 vaccine, which has larger efficacy, is always indicated, while the use of the V_2 vaccine decreases.

Finally, for vaccines V_1 with 74% efficacy and V_2 with 67% efficacy, we will see in Figure 18 the curves of infected people in three contexts: when we only use the V_1 vaccine, when we use both vaccines according to the optimal control in Figure 13, and when we only use the V_2 vaccine.

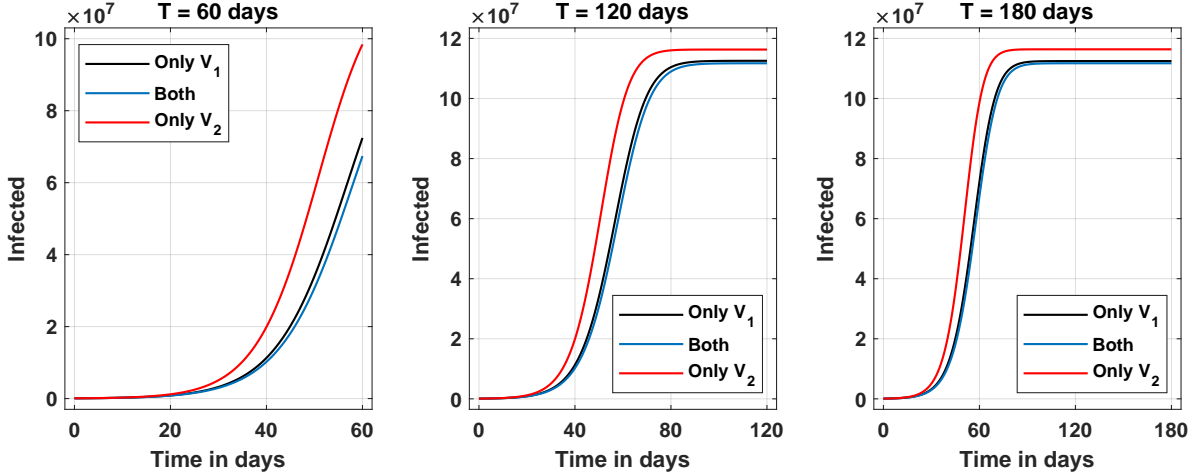


Figure 18: Curves of infected for different use of the vaccines.

Analyzing Figure 18, we highlight the economic importance of optimal control. When we use only the V_2 vaccine, we have the lowest possible cost, but there is a considerable increase in the number of infected people compared to the other two strategies. Note that the infected curve exhibits practically the same behavior when we use both vaccines or when we use only the V_1 vaccine, which is more effective and has the most expensive implementation for the government. In this case, the strategy of using both vaccines, as defined by optimal control, presents a slight reduction in the number of infected people, with an affordable cost.

5 Conclusions

In this paper, we considered a SEIR model adapted for a vaccination campaign with two types of vaccines, V_1 and V_2 . The controls of the system are the usage parameters of the vaccines. We found the optimal controls via Pontryagin's maximum principle and used the forward-backward sweep method, to calculate the controls numerically.

Throughout the paper, we utilized four values for the efficacy of the vaccines: 91%, 74%, 67%, 51%, and investigated the optimal controls for each pair of these values. Based on what was indicated by the optimal control, we showed how the procurement of vaccines should be distributed and how they should be used. When the efficacy values were very similar, we presented a sensitivity analysis for the parameters. Furthermore, we showed how the simultaneous use of the two vaccines, according to the optimal control, reduces the number of infected individuals at a more affordable cost.

When the V_2 vaccine is 51% effective, the use of the other vaccine with efficacy greater than or equal to 67% is indicated, i.e., a 51% effective vaccine is only recommended when it is the only option available. We understand that this occurs due to the effect of efficacy on the transmission rate, which decreases linearly. The V_2 vaccine has a transmission rate that is considered high when compared to the rates of other vaccines.

When considering the V_1 vaccine with 91% efficacy and the V_2 vaccine with 74% or 67% efficacy, the use of the vaccine with higher efficacy is indicated almost all the time, followed by a simultaneous use of both vaccines during the last days of the campaign. This likely occurs to balance economic expenses, as the population can achieve collective immunity. The distribution for the purchase of vaccines indicated that in general more than 93% of the vaccines utilized must be from the V_1 vaccine.

When the V_1 vaccine is 74% effective and the V_2 vaccine is 67% effective, the optimal control indicated a simultaneous use throughout the entire campaign. In this case, the procurement of both vaccines is recommended. In the sensitivity analysis of the recovery rate and the rate of returning to the susceptible class, the control of simultaneous use only changes when the recovery rate of the V_2 vaccine and the rate of returning to the susceptible class of the V_1 vaccine decrease by 20%. In this scenario, for all campaigns lengths, the exclusive use of the vaccine with higher efficacy is indicated for approximately the first 30 days, followed by simultaneous use until the end of the campaign. The purchase should consist of approximately 70% of the V_1 vaccine and 30% of the V_2 vaccine. For the sensitivity of efficacy values, when the V_2 vaccine is fixed with efficacy of 67%, the scenario of simultaneous use only changes when the V_1 vaccine has efficacy above 77%. Conversely, when the V_1 vaccine is fixed with 74% of efficacy, the scenario of

simultaneous use is only not indicated when the V_2 vaccine has efficacy lower than 65%. When these changes occurs, it is recommended to use only the V_1 vaccine for an initial period, followed by simultaneous use.

Finally, we also observed that the context in which simultaneous use is indicated by optimal control throughout the entire campaign presents a smaller number of infected individuals when compared with the contexts in which only one vaccine is used, and this minimizes economic costs.

We conclude that unless we have a vaccine with very low effectiveness (e.g., 51%, for which use is not indicated) or two vaccines with very similar efficacy (for which simultaneous use is indicated at all times), the optimal controls indicate a standard behavior: initial use of the more effective vaccine only, followed by simultaneous use.

In our model, we utilized COVID-19 data from Brazil for the initial conditions and data from the literature for parameter values. This type of study can be conducted to investigate vaccination campaigns for other diseases by adapting the model according to their characteristics and using initial conditions that suit the specific context (for example, Brazil is very large, and there may be underreporting and other factors that introduce noise in the data), followed by appropriate estimation of the parameters.

Acknowledgements

The first author was partially supported by CAPES, Brazil.

References

- [1] Gerardo Chowell, Lisa Sattenspiel, Shweta Bansal, and Cécile Viboud. Mathematical models to characterize early epidemic growth: A review. *Physics of Life Reviews*, 18:66–97, 2016.
- [2] Richard Horton. *The COVID-19 Catastrophe: What’s Gone Wrong and How to Stop it Happening Again*. Polity Press, Cambridge, 2020.
- [3] Walter A. Orenstein and Rafi Ahmed. Simply put: Vaccination saves lives. *Proceedings of the National Academy of Sciences*, 114(16):4031–4033, 2017.
- [4] Oliver J Watson, Gregory Barnsley, Jaspreet Toor, Alexandra B Hogan, Peter Winskill, and Azra C Ghani. Global impact of the first year of covid-19 vaccination: a mathematical modelling study. *The Lancet Infectious Diseases*, 22:1293–1302, 2022
- [5] Xianning Liu, Yasuhiro Takeuchi, and Shingo Iwami. Svir epidemic models with vaccination strategies. *Journal of Theoretical Biology*, 253(1):1–11, 2008.
- [6] M. E. Alexander, C. Bowman, S. M. Moghadas, R. Summers, A. B. Gumel, and B. M. Sahai. A vaccination model for transmission dynamics of influenza. *SIAM Journal on Applied Dynamical Systems*, 3(4):503–524, 2004.
- [7] Franklin Agouanet Leontine Nkague Nkamba, Thomas Timothee Manga and Martin Luther Mann Manyombe. Mathematical model to assess vaccination and effective contact rate impact in the spread of tuberculosis. *Journal of Biological Dynamics*, 13(1):26–42, 2019.
- [8] Jemal Mohammed-Awel, Eric Numfor, Ruijun Zhao, and Suzanne Lenhart. A new mathematical model studying imperfect vaccination: Optimal control analysis. *Journal of Mathematical Analysis and Applications*, 500(2):125132, 2021.
- [9] Burcu Balcik, Ecem Yucesoy, Berna Akca, Sirma Karakaya, Asena A. Gevsek, Hossein Baharmand, and Fabio Sgarbossa. A mathematical model for equitable in-country covid-19 vaccine allocation. *International Journal of Production Research*, 60(24):7502–7526, 2022.
- [10] Kate M. Bubar, Kyle Reinholt, Stephen M. Kissler, Marc Lipsitch, Sarah Cobey, Yonatan H. Grad, and Daniel B. Larremore. Model-informed covid-19 vaccine prioritization strategies by age and serostatus. *Science*, 371(6532):916–921, 2021.
- [11] Sam Moore, Edward M Hill, Louise Dyson, Michael J Tildesley, and Matt J Keeling. Vaccination and nonpharmaceutical interventions for covid-19: a mathematical modelling study. *The Lancet Infectious Diseases*, 21:793–802, 2021.
- [12] Alberto Olivares and Ernesto Staffetti. Uncertainty quantification of a mathematical model of covid-19 transmission dynamics with mass vaccination strategy. *Chaos, Solitons & Fractals*, 146:110895, 2021.
- [13] James Nicodemus Paul, Isambi Sailon Mbalawata, Silas Steven Mirau, and Lemjini Masandawa. Mathematical modeling of vaccination as a control measure of stress to fight covid-19 infections. *Chaos, Solitons & Fractals*, 166:112920, 2023.

- [14] Charlene MC Rodrigues and Stanley A Plotkin. Impact of vaccines; health, economic and social perspectives. *Frontiers in microbiology*, 11:1526, 2020.
- [15] James Ryan, York Zoellner, Birgit Gradl, Bram Palache, and Jeroen Medema. Establishing the health and economic impact of influenza vaccination within the european union 25 countries. *Vaccine*, 24(47-48):6812–6822, 2006.
- [16] Jenifer Ehreth. The global value of vaccination. *Vaccine*, 21(7-8):596–600, 2003.
- [17] Hem Raj Joshi. Optimal control of an hiv immunology model. *Optimal control applications and methods*, 23(4):199–213, 2002.
- [18] K Renee Fister, Suzanne Lenhart, and Joseph Scott McNally. Optimizing chemotherapy in an hiv model. *Electronic Journal of Differential Equations*, 1998.
- [19] Denise Kirschner, Suzanne Lenhart, and Steve Serbin. Optimal control of the chemotherapy of hiv. *Journal of mathematical biology*, 35:775–792, 1997.
- [20] Cristiana J Silva and Delfim FM Torres. Optimal control for a tuberculosis model with reinfection and postexposure interventions. *Mathematical Biosciences*, 244(2):154–164, 2013.
- [21] Eunok Jung, Suzanne Lenhart, and Zhilan Feng. Optimal control of treatments in a two-strain tuberculosis model. *Discrete and Continuous Dynamical Systems Series B*, 2(4):473–482, 2002.
- [22] Sunmi Lee, Gerardo Chowell, and Carlos Castillo-Chávez. Optimal control for pandemic influenza: the role of limited antiviral treatment and isolation. *Journal of Theoretical Biology*, 265(2):136–150, 2010.
- [23] Horst Behncke. Optimal control of deterministic epidemics. *Optimal control applications and methods*, 21(6):269–285, 2000.
- [24] Joaquim P Mateus, Paulo Rebelo, Silvério Rosa, César M Silva, and Delfim FM Torres. Optimal control of non-autonomous seirs models with vaccination and treatment. *arXiv preprint arXiv:1706.06843*, 2017.
- [25] Ramses Djidjou-Demasse, Yannis Michalakis, Marc Choisy, Micea T Sofonea, and Samuel Alizon. Optimal covid-19 epidemic control until vaccine deployment. *MedRxiv*, pages 2020–04, 2020.
- [26] Zhong-Hua Shen, Yu-Ming Chu, Muhammad Altaf Khan, Shabbir Muhammad, Omar A Al-Hartomy, and M Higazy. Mathematical modeling and optimal control of the covid-19 dynamics. *Results in Physics*, 31:105028, 2021.
- [27] Legesse Lemecha Obsu and Shiferaw Feyissa Balcha. Optimal control strategies for the transmission risk of covid-19. *Journal of biological dynamics*, 14(1):590–607, 2020.
- [28] Muhammad Zamir, Thabet Abdeljawad, Fawad Nadeem, Abdul Wahid, and Ali Yousef. An optimal control analysis of a covid-19 model. *Alexandria Engineering Journal*, 60(3):2875–2884, 2021.
- [29] João A.M. Gondim and Larissa Machado. Optimal quarantine strategies for the covid-19 pandemic in a population with a discrete age structure. *Chaos, Solitons & Fractals*, 140:110166, 2020.
- [30] N.L Santos Junior and Joao AM Gondim. Optimal screening strategies in the control of an infectious disease: a case of the covid-19 in a population with age structure. *arXiv preprint arXiv:2411.00312*, 2024.
- [31] Sarah M. Bartsch, Kelly J. O’Shea, Marie C. Ferguson, Maria Elena Bottazzi, Patrick T. Wedlock, Ulrich Strych, James A. McKinnell, Sheryl S. Siegmund, Sarah N. Cox, Peter J. Hotez, and Bruce Y. Lee. Vaccine efficacy needed for a covid-19 coronavirus vaccine to prevent or stop an epidemic as the sole intervention. *American Journal of Preventive Medicine*, 59(4):493–503, 2020.
- [32] Monia Makhoul, Houssein H. Ayoub, Hiam Chemaitelly, Shaheen Seedat, Ghina R. Mumtaz, Sarah Al-Omari, and Laith J. Abu-Raddad. Epidemiological impact of sars-cov-2 vaccination: Mathematical modeling analyses. *Vaccines*, 8(4), 2020.
- [33] K. Tentori, A. Passerini, B. Timberlake, and S. Pighin. The misunderstanding of vaccine efficacy. *Social Science & Medicine*, 289:114273, 2021.
- [34] M. Martcheva. *An Introduction to Mathematical Epidemiology*. Texts in Applied Mathematics. Springer US, 2015.
- [35] WHO. Interim recommendations for use of the pfizer biontech covid 19 vaccine bnt162b2 , under emergency use listing. *World Health Organization*, 2022.
- [36] WHO. Interim recommendations for use of the chadox1-s [recombinant] vaccine against covid-19 (astrazeneca covid-19 vaccine azd1222 vaxzevria™, sii covishield™). *World Health Organization*, 2022.
- [37] WHO. Interim recommendations for the use of the janssen ad26.cov2.s (covid-19) vaccine. *World Health Organization*, 2022.

-
- [38] WHO. Interim recommendations for use of the inactivated covid-19 vaccine, coronavac, developed by sinovac. *World Health Organization*, 2022.
- [39] Victoria Hall, Sarah Foulkes, Ferdinando Insalata, Peter Kirwan, Ayoub Saei, Ana Atti, Edgar Wellington, Jameel Khawam, Katie Munro, Michelle Cole, et al. Protection against sars-cov-2 after covid-19 vaccination and previous infection. *New England Journal of Medicine*, 386(13):1207–1220, 2022.
- [40] Sezanur Rahman, M Mahfuzur Rahman, Mojnu Miah, Mst Noorjahan Begum, Monira Sarmin, Mustafa Mahfuz, Mohammad Enayet Hossain, Mohammed Ziaur Rahman, Mohammad Jobayer Chisti, Tahmeed Ahmed, et al. Covid-19 reinfections among naturally infected and vaccinated individuals. *Scientific reports*, 12(1):1438, 2022.
- [41] Aisha Fakhroo, Hebah A. AlKhatib, Asmaa A. Al Thani, and Hadi M. Yassine. Reinfections in covid-19 patients: Impact of virus genetic variability and host immunity. *Vaccines*, 9(10), 2021.
- [42] Ghassan Hamra, Richard MacLehose, and David Richardson. Markov chain monte carlo: an introduction for epidemiologists. *International journal of epidemiology*, 42(2):627–634, 2013.
- [43] Worldmeters, 2024. Accessed on April 26, 2024.
- [44] Stephen A. Lauer, Kyra H. Grantz, Qifang Bi, and et al. The incubation period of coronavirus disease 2019 (covid-19) from publicly reported confirmed cases: Estimation and application. *Annals of Internal Medicine*, 172(9):577–582, 2020.
- [45] Hem Raj Joshi, Suzanne Lenhart, Michael Y Li, and Liancheng Wang. Optimal control methods applied to disease models. *Contemporary Mathematics*, 410:187–208, 2006.
- [46] L.S. Pontryagin. *Mathematical Theory of Optimal Processes*. Routledge, 2018.
- [47] S. Lenhart and J.T. Workman. *Optimal Control Applied to Biological Models*. Chapman and Hall/CRC, 2007.
- [48] S. Chapra, *Applied Numerical Methods with MATLAB for Engineers and Scientists*, McGraw-Hill Education, 2018.